

**Io's Neutral Clouds: From the Atmosphere to the
Plasma Torus**

by

Matthew Howard Burger

M. S., Astrophysical and Planetary Sciences, University of
Colorado

B. A., Physics, Rice University

A thesis submitted to the
Faculty of the Graduate School of the
University of Colorado in partial fulfillment
of the requirements for the degree of
Doctor of Philosophy

Department of Astrophysical and Planetary Sciences

2006

This thesis entitled:
Io's Neutral Clouds: From the Atmosphere to the Plasma Torus
written by Matthew Howard Burger
has been approved for the Department of Astrophysical and Planetary Sciences

Professor Nicholas M. Schneider

Professor Fran Bagenal

Date _____

The final copy of this thesis has been examined by the signatories, and we find that both the content and the form meet acceptable presentation standards of scholarly work in the above mentioned discipline.

Burger, Matthew Howard (Ph. D., Planetary Science)

Io's Neutral Clouds: From the Atmosphere to the Plasma Torus

Thesis directed by Professor Nicholas M. Schneider

Since the discovery of sodium thirty years ago, observations of Io's neutral features have provided essential insight into understanding the relationship between the Io's atmosphere and the Io torus, a ring of plasma encircling Jupiter. In this thesis I use observations and models of Io's corona, extended neutral clouds, and fast sodium jet to probe the interactions between the atmosphere, torus, and neutral clouds.

A corona and neutral cloud model, based on the model of Wilson and Schneider (1999), has been developed to study neutral loss from Io. Neutrals are ejected from Io's exobase and their trajectories followed under the influence of gravity until lost into the plasma torus. I also developed description of the plasma torus based on Voyager and ground-based observations to accurately determine neutral lifetimes.

Mutual eclipsing events between Galilean satellites were used to measure the shape of Io's sodium corona, revealing a corona that is only approximately spherically symmetric around Io. I discovered a previously undetected asymmetry: the sub-Jupiter corona is denser than the anti-Jupiter corona. Modeling implies that sodium source from the sub-Jupiter hemisphere must be twice as large as from the anti-Jupiter hemisphere.

The Galileo spacecraft has imaged a remarkable atmospheric escape process occurring in Io's ionosphere. Electrodynamic consequences of Io's motion through Jupiter's magnetosphere drive mega-amp currents through Io's ionosphere; some sodium ions carrying this current are neutralized as they leave the atmosphere. The Galileo images show that the resulting fast sodium jet removes $\sim 5 \times 10^{25}$ atoms sec^{-1} from Io's atmosphere. The source region of the jet is much smaller than Io itself implying that the ionosphere is densest near Io's equator.

A model-based comparison of the neutral oxygen and sodium clouds details differences in the morphologies and spatial extent of each: sodium extends only 1/4 the way around Jupiter while oxygen forms a complete torus. Sodium emission results from resonant scattering making it relatively easy to determine sodium abundance. The oxygen intensity is highly dependent on the highly variable plasma torus. This complicates the analysis of oxygen observations since the the nature and magnitude of plasma variations has not been well characterized.

Dedication

To Rachel, despite the fact that she made me finish.

Acknowledgements

First let me thank Boulder: if I had to be stuck in grad school for seven years somewhere, Boulder was a good place for it.

Thanks to Nick Schneider for his seven years of advising, guidance, patience, and sending me to the telescope with reasonable regularity.

Thanks to Fran Bagenal for pushing me along and letting me know when it was good enough.

Also, my additional committee members deserve recognition for reading through the whole thing and their insightful comments and questions: Bob Ergun, Mihaly Horanyi, and Ian Stewart (who deserves extra thanks for being a last minute addition to the group). Also thanks to Peter Delamere for agreeing to be on the committee even if his services were not taken advantage of.

I have received observing assistance and data from a number of observers including Imke de Pater, Mike Brown, Antonin Bouchez, Anthony Mallama, Larry Trafton, and Yaron Scheffer all of whom provided me with the mutual event data from Keck and McDonald Observatories. Also, I wish to acknowledge Don Hunten, Ann Sprague, Rik Hill for help and instruction using the LPL Echelle and Coronagraph at Catalina Observatory, as well as their often heroic efforts to repair the instruments during observing runs.

I have received help and guidance from many people through these years from colleagues at other institutions. In particular I'd like to mention Jody Wilson for al-

lowing me to dissect and reassemble his model, as well as an endless enthusiasm for observing sodium. Melissa McGrath has also provided encouragement and support at the times I needed it most.

Thanks to David Brain for seven years of office sharing, protecting my office space while I was off in Virginia, and trying not to wake me up during my many naps of the couch.

And lastly Rachel Osten deserves extra acknowledgment for spending Thanksgiving 1999 and Christmas 2000 alone on a mountain observing with me, reading over the entire thesis, and forcing me to finish it even when I didn't really want to.

Table of Contents

Chapter

1	Introduction	1
1.1	Io's Atmosphere	1
1.2	Observations of the Corona and Neutral Clouds	3
1.3	Neutral Cloud Models	7
1.4	Organization of the Thesis	10
2	Physical Processes Governing Neutrals	13
2.1	Introduction	13
2.2	Emission and Absorption Mechanisms	13
2.2.1	Resonant Scattering: Observing Sodium	14
2.2.2	Electron Impact Excitation: Observing oxygen and sulfur	20
2.3	Creating the neutral clouds: Sputtering	21
2.4	Destruction Physics	25
2.4.1	Electron Impact ionization	26
2.4.2	Charge exchange	28
2.5	Neutral Dynamics	29
2.5.1	Gravity	29
2.5.2	Radiation Pressure	31
2.6	Summary	32

3	Io's Corona: Creation and Destruction	34
3.1	Introduction	34
3.2	Observations	35
3.2.1	Keck Observatory Observations	38
3.2.2	McDonald Observatory Observations	42
3.2.3	Catalina Observatory Observations	43
3.3	Analysis	43
3.4	Discussion	49
3.5	Summary	59
4	Galileo Observations of the Fast Sodium Jet	61
4.1	Introduction	61
4.2	Observations	64
4.3	Analysis	65
4.4	Discussion	66
5	Io's Escaping Neutrals	71
5.1	Introduction	71
5.2	Previous Neutral Cloud Models	73
5.3	A Model of Io's Neutral Clouds	74
5.3.1	Description of the model	74
5.3.2	Treatment of the Io Plasma Torus	77
5.3.3	Neutral Lifetimes in the Inner Jovian System	90
5.3.4	Flux Distributions	97
5.4	Basic Tests of the Neutral Cloud model	99
5.4.1	Effect of Radiation Pressure	99
5.4.2	Testing the model: East/West Sodium Brightness Asymmetry .	101
5.4.3	Testing the model: North/South Sodium Brightness Asymmetry	103

5.5	Summary	105
6	Modeling Io's Corona	108
6.1	Introduction	108
6.2	Description and Analysis of Model Runs	110
6.3	Understanding the Shape of the Corona	112
6.3.1	The Average Observed Corona	112
6.3.2	Variations in the Average Corona	120
6.3.3	Building to an Offset Tilted Dipole with an East/West Electric Field	121
6.3.4	Effect of Uniform Variations in the Torus on the Corona	125
6.3.5	Effect of Magnetic Longitude Variations on the Corona	131
6.4	Understanding the Inner/Outer Asymmetry in the Corona	134
6.5	Io's Oxygen Corona	141
6.5.1	Observations	142
6.5.2	The Average Oxygen Corona	144
6.5.3	The Oxygen Asymmetry	148
6.6	Summary	150
7	Io's Extended Neutral Clouds	154
7.1	Introduction	154
7.2	Neutral Cloud Models	155
7.3	Large Scale Features	158
7.3.1	Motions of Neutral Atoms	158
7.3.2	Loss of Neutral Atoms	166
7.3.3	Neutral Cloud Brightnesses	167
7.4	Observations of the Sodium Neutral Cloud	180
7.5	Summary	182

8	Conclusions	184
8.1	Summary of the Thesis	184
8.2	Major Results	186
	Bibliography	190
A	Summary of Eclipse Observations	197
	Appendix	
B	Transformation to the Plasma Coordinate System	202

List of Tables

Table

2.1	Sodium D Line Parameters	17
2.2	Summary of neutral lifetimes for ionization processes	28
2.3	Neutral-Ion charge exchange reactions	30
3.1	Eclipse Parameters	39
6.1	Comparison of corona created with different cross sections, different ejection direction distribution, and different models	116
6.2	Summary of oxygen corona observed by Wolven et al. (2001).	144
7.1	Summary of all available sodium images	181
A.1	Summary of Eclipse Observations	198
A.1	Summary of Eclipse Observations	199
A.1	Summary of Eclipse Observations	200
A.1	Summary of Eclipse Observations	201

List of Figures

Figure

1.1	Discovery of sodium at Io by Brown (1974).	5
1.2	Sunlight available for resonant scattering	9
2.1	Schematic of sodium D resonance line transitions	15
2.2	Curves of growth for sodium D ₂ line	18
2.3	Cartoon of cascade sputtering	22
2.4	Sputtering Flux Distribution	24
2.5	Electron impact ionization cross sections and rate coefficients	27
3.1	Io eclipsing Europa	36
3.2	Removal of solar spectrum	37
3.3	Io's orbital geometry during mutual events	40
3.4	Determination of Impact Parameters	45
3.5	Equivalent widths during mutual events	47
3.6	Determination of corona temperature and column density	48
3.7	Corona column density profile	50
3.8	Mutual event eclipse geometry	53
3.9	Equivalent width vs. Impact parameter	54
3.10	Column density asymmetry in the corona	55
4.1	Cartoon of directional feature geometry	63

4.2	Io's sodium jet through Galileo's clear and green filters	67
4.3	Comparison of Galileo data and modeled jet images	69
5.1	Model Coordinate System	76
5.2	Cartoon of Jupiter's dipole magnetic field	79
5.3	Electron density and temperature in the centrifugal equator	80
5.4	Observations of the Ribbon by Schneider and Trauger (1995)	81
5.5	Illustration of the importance of line-of-sight effects in ground-based ob- servations of the plasma torus	83
5.6	Io's location in the plasma torus at all magnetic and orbital longitudes .	85
5.7	Neutral lifetimes in the inner Jovian system for different loss processes .	91
5.8	Neutral lifetimes at Io for the basic torus model	93
5.9	Neutral lifetimes at Io for the varying torus model	94
5.10	Comparison of sodium lifetime in the corona predicted by this work with Smyth and Combi (1988b)	96
5.11	Fraction of atoms with escape velocity for different flux distributions. . .	98
5.12	Effect of radiation pressure on sodium in the cloud and corona.	100
5.13	Model of the East/West Sodium Brightness Asymmetry	102
5.14	Demonstration of the north/south sodium cloud asymmetry	104
6.1	Modeled image of the corona with radial profile	111
6.2	Radially averaged models of a sputtered corona	113
6.3	Radially averaged models of a corona with an exponential source distri- bution	114
6.4	Motion and ionization of sodium atoms in the corona.	119
6.5	Effects of Jupiter's offset tilted dipole and the east/west electric field on the corona	122

6.6	Demonstration of the effect of the east/west electric field on sodium emission from the corona.	124
6.7	Effect of uniformly varying torus electron density on the sodium corona.	126
6.8	Effect of uniformly varying torus ion temperature on the sodium corona.	129
6.9	Effect of variations in the strength of the east/west electric field on the corona.	132
6.10	Effect of magnetic longitude variations in the torus on the shape of the corona.	133
6.11	Sketch of the regions about Io for discussing the corona asymmetry. . .	136
6.12	Shape of the corona when the source is limited to a single hemisphere. .	137
6.13	Shape of the corona using combinations of sputtering from each side of Io.	138
6.14	Shape of the corona allowing the most probable velocities of each hemisphere to vary independently.	140
6.15	Example of STIS image of Io's atmospheric emissions	143
6.16	Power law slope in the oxygen corona as function of most probable velocity.	145
6.17	Fraction of atoms escaping from Io's corona as function of neutral lifetime and initial velocity.	147
6.18	Effect of electron temperature variations near Io on the coronal oxygen intensity profile.	149
7.1	Examples of modeled oxygen and sodium clouds	157
7.2	Decomposition of model image into observable quantities.	159
7.3	Sample trajectories of neutral atoms ejected from Io	161
7.4	Streamlines of atoms ejected from Io.	162
7.5	Illustration of atoms without escape velocity escaping from Io	163
7.6	Intermediate scale view of neutrals escaping Io	165
7.7	Neutral lifetime as function of the modified L-shell	168

7.8	Examples of modeled neutral cloud brightnesses	169
7.9	Observable changes in the sodium cloud due to Io's motion	171
7.10	Observable changes in the sodium corona due to Io's motion	172
7.11	Comparison between brightness and column density profiles of the sodium neutral cloud.	174
7.12	Effect of the tilt of Jupiter's equatorial plane relative to Earth.	176
7.13	Observable changes in the oxygen cloud due to the changing plasma torus geometry	177
7.14	Variation in oxygen cloud brightness due to torus variability.	178

Chapter 1

Introduction

Io was a simple country nymph who caught Jupiter's eye. Jupiter's wife Juno, suspicious of Jupiter's intentions toward Io, came down to investigate. Jupiter acted quickly by turning Io into a cow. Juno complimented Jupiter on having such a nice cow and asked if she could have it. Because Juno would be suspicious if he refused to give her something so simple as a cow, Jupiter had no choice but to relinquish Io.

Juno was still suspicious of Jupiter and his "cow," so she told Argus, the hundred-eyed creature, to watch over Io. Eventually, Jupiter began to feel guilty about what he had done to Io, so he sent Mercury to kill Argus. Mercury did this, so Jupiter was able to change Io back to her original form.

In this thesis, I use the the watchfulness of Argus and Juno-like models to try to understand the interactions of Io and Jupiter. We must hope that she is revealed before all the observers are gone. (Paraphrased from *Metamorphoses*, Ovid).

1.1 Io's Atmosphere

The first observational evidence of an atmosphere at Io were measurements made by Binder and Cruikshank (1964) who showed an increase in Io's albedo immediately after emerging from eclipse which then decreased to its pre-eclipse value over several hours. This brightening was interpreted as an atmosphere condensing out when solar heating is turned off, creating a reflective surface frost layer that sublimates when the sun

heats the surface after eclipse. Although this observation has only been intermittently repeated since then and remains somewhat controversial, it is now known that Io does in fact have an atmosphere which at least partially condenses when Io goes into eclipse (see reviews by Lellouch (1996); Spencer and Schneider (1996)).

The existence of this atmosphere, however, was still unproven for a decade after Binder and Cruickshank's observations. The Pioneer 10 radio-occultation experiment detected Io's ionosphere (Kliore et al. 1974, 1975), providing more definitive indirect evidence for the atmosphere. At about the same time, sodium emission from Io was discovered by Brown (1974). Sodium has since proved to be minor in abundance but extremely important for studying the dominant species (Section 1.2).

The Voyager flybys of Jupiter propelled Io to a new level of respect in the scientific community with their discovery of the only known extra-terrestrial volcanism. Voyager also made the first direct observation of Io's near-surface atmosphere with a spectrum of SO_2 (Pearl et al. 1979). As only sodium and potassium (discovered by Trafton (1975b)) were known to originate from Io previous to Voyager, and these had been observed in extended clouds extending large distances from Io but not in a near-surface atmosphere, the discovery of this most abundant species in Io's atmosphere provided a new direction for atmospheric studies.

With the passing of Voyager from Jupiter, no detections of Io's atmosphere were made for over a decade Lellouch et al. (1990). The 1980s were spent trying to understand the single SO_2 observation from Voyager. Three classes of models were developed for understanding the atmosphere: buffered models (e.g., Kumar (1982) assume the SO_2 atmosphere is in vapor pressure equilibrium with the surface frost; volcanic models (Ingersoll 1989; Moreno et al. 1991) consider an atmosphere supplied by local volcanic sources; and sputtering models (Sieveka and Johnson 1984) look at an atmosphere created by charged particle impact on the surface.

Observations in the mid-1990s helped to clarify the global extent of the atmo-

sphere. Images of Io passing in front of Jupiter detected absorption by SO_2 and S_2 in a plume silhouetted against Io’s disk (Spencer et al. 1997, 2000), proving that the sulfur dioxide is contained in some volcanic emissions. The presence of a global atmosphere has been suggested by observations which detected gaseous SO_2 above three distinct geographical regions on Io’s surface (McGrath et al. 2000).

Recently, the *Hubble Space Telescope* has provided an exciting new technique for observing Io’s atmospheric SO_2 (Roesler et al. 1999; Feldman et al. 2000). Images of Io’s SO_2 distribution are obtained with the Space Telescope Imaging Spectrograph (STIS) by making spatially resolved observations of solar Lyman- α reflected off Io’s surface due to attenuation by SO_2 in Io’s atmosphere. These images show a global but non-uniform and time-variable atmosphere with SO_2 gas concentrated near Io’s equator. Results from the Galileo spacecraft support this suggestion with observations indicating that Io has a global ionosphere (Hinson et al. 1998). Evidence is presented in Chapter 4 that the ionosphere may be denser near the equator.

1.2 Observations of the Corona and Neutral Clouds

The focus of this thesis is not Io’s near-surface atmosphere but the features formed from the escape of this atmosphere. Using thirty years of observations, sodium is known to escape through “slow” and “fast” processes. Sputtering of neutrals off the atmosphere and surface form the extended cloud: a banana shaped cloud of slowly escaping neutrals (mean velocity $\sim 2 - 3 \text{ km s}^{-1}$ with a high speed tail extending to $\sim 10 - 30 \text{ km s}^{-1}$) which primarily leads Io in its orbit around Jupiter (Smyth 1992). Similar clouds exist for the more dominant species of sulfur and oxygen (Brown 1981a; Thomas 1996), but have not been well studied since emission from these species are at the limits of what can be observed. There are several mechanisms which result in the escape of fast sodium (velocity $\gtrsim 10 \text{ km s}^{-1}$). Jupiter’s magnetic field accelerates sodium ions in Io’s collisionally thick ionosphere which are neutralized through charge exchange

to produce fast neutrals (Wilson and Schneider 1999). Sodium ions in the plasma torus can also charge exchange with neutrals to create fast sodium. Similarly, sodium-bearing molecular ions are swept into the torus of plasma which encircles Jupiter and dissociation of these molecules creates a separate fast sodium feature (Wilson and Schneider 1994). Additional fast sodium results from the high speed tail of the sputtering flux distribution (Smyth 1992). A short summary of the observational and modeling efforts to understand Io's neutral features follows.

Since its discovery thirty years ago (Brown (1974), Figure 1.1), sodium has proved itself to be essential for understanding the escape of Io's atmosphere. Despite its small abundance, optical wavelength observations of sodium have several advantages over observations of more abundant species such as oxygen and sulfur. The emission from these species results from electron impact excitation in the plasma torus, so the observed emission is a function of both the neutral density and the electron density and temperature of the plasma, making the neutral density profile difficult to determine from observational data without detailed modeling. Even in regions where the plasma is less important for creating the emission, the lines are weak and at wavelengths inaccessible from the ground. Because the sodium D lines are formed through a resonant transition at optical wavelengths, sodium can be observed at Io in both emission and absorption when in sunlight. Also, sodium emission is much brighter than optical emissions from other atmospheric components.

The observations of sodium made within a few years of its discovery fleshed out the spatial extent and general morphology of the cloud. Using separate spectra of Io's disk and the region near Io's disk, Trafton et al. (1974) demonstrated that the emission originates from an extended region at least $10''$ ($\sim 20 R_{\text{Io}}$) in radius around Io. Continued observations of the spatial extent of the cloud detected a partial torus of neutral sodium extending at least one-fifth of the way around Jupiter from Io (Macy and Trafton 1975b). The first two-dimensional images of the cloud (Muench and Bergstralh

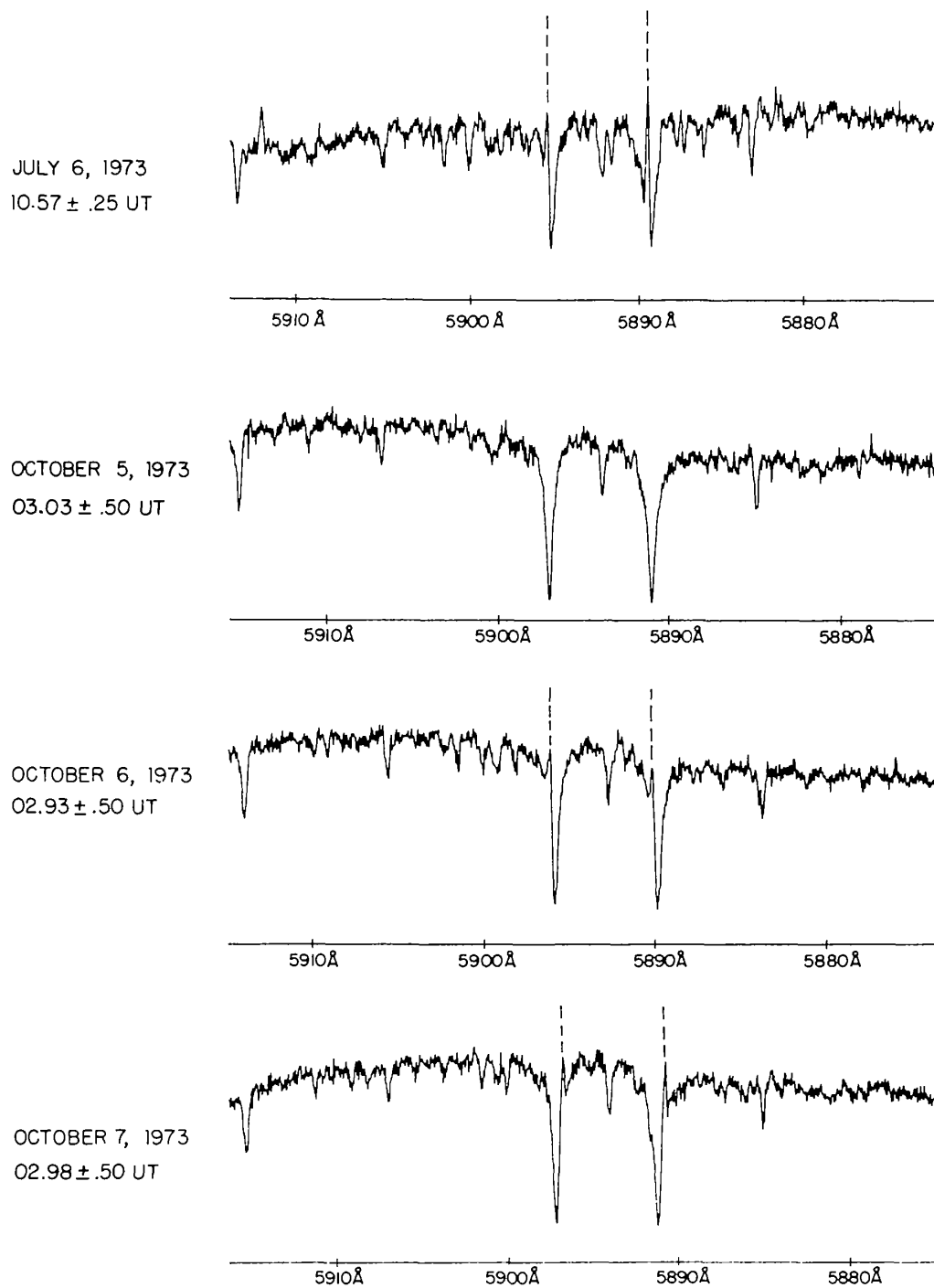


Figure 1.1 The earliest spectra of Io's sodium emission by Brown (1974). Iogenic sodium D lines are indicated with broken lines. These spectra are reproduced from Brown and Chaffee (1974)

1977; Matson et al. 1978; Murcray and Goody 1978) showed the “banana-shaped” cloud primarily leading Io in its orbit.

Because several groups were involved in monitoring programs and other observations of the sodium emission, two asymmetries were discovered even while the general morphology of the cloud was still being determined. Bergstralh et al. (1975, 1977) demonstrated that although on average the sodium emission remains roughly constant from one year to the next, the intensity is about 25% higher when Io is at eastern elongation (orbital phase = 90°) than at western elongation (orbital phase = 270°). This is in addition to an approximately 20% variation in the overall brightness which did not correlate with any known variables (e.g. Io’s magnetic longitude). A north/south asymmetry was discovered by Trafton and Macy (1975): the ratio of the sodium brightness north of Io to that south of Io is a function of Io’s magnetic longitude with the side further from the magnetic equator showing brighter emission. The discovery of the plasma torus by Voyager in 1979 provided an explanation for this asymmetry (Trafton 1980).

Neutral clouds of other species have also been detected. Trafton (1975b) discovered potassium originating from Io with a morphology similar to the sodium cloud. Although oxygen and sulfur are the most abundant species in the cloud, observations of each have been sparse: Oxygen was discovered by Brown (1981b); sulfur by Durrance et al. (1983). Recent years have also seen a monitoring program of optical wavelength emissions of neutral oxygen at 6300 \AA originating near Io’s disk (Scherb and Smyth 1993; Oliverson et al. 2001).

Although spectroscopic and imaging studies were able to study the morphology of the large scale features, it was not possible to observe sodium in Io’s corona close to Io. The corona, or exosphere, is the region within $\sim 6 R_{\text{Io}}$ consisting of bound and escaping atoms which have been lost from Io’s collisional atmosphere but are still in the region where Io’s gravity dominates over Jupiter’s. In general, it is not possible to spatially resolve the region close to Io because of Io’s high geometric albedo and the

effects of atmospheric seeing. Observations of Io eclipsing the other Galilean satellites (Schneider et al. 1987, 1991a) however, has provided a method of determining the radial column density profile of sodium close to Io. Additionally, the HST observations which produced the images of Io’s atmospheric SO₂, have also measured the radial intensity profiles of oxygen and sulfur in Io’s corona for the first time (Wolven et al. 2001).

The early spectra also detected a fast component to the sodium escaping from Io (Trafton 1975a). Sodium has since been observed at speeds of up to 100 km s⁻¹ Brown (1981a). Early imaging studies of the fast sodium features (Goldberg et al. 1984; Pilcher et al. 1984) characterized it as a narrow feature directed away from Jupiter perpendicular to the Jovian magnetic field line through Io. A second fast sodium feature, known as the molecular ion stream, was discovered by Schneider et al. (1991b) and originates in the plasma torus. This feature has been shown to result from dissociation of molecular ions in the torus (Schneider et al. 1991b; Wilson and Schneider 1994).

1.3 Neutral Cloud Models

Modeling efforts to understand Io’s sodium emission began almost immediately after its discovery. These earliest models concentrated on understanding the basic source, loss, and emission mechanisms to great success. Matson et al. (1974) made the first prediction that sodium atoms sputtered are the source of the cloud of sodium around Io.

The first attempt to understand the emission mechanism was made by McElroy et al. (1974) who assumed that Io has a “normal” satellite atmosphere consisting of nitrogen gas with a trace sodium component excited by collisions with N₂. Resonant scattering of sunlight by sodium atoms was initially ruled out due to energy requirements and the assumption that sodium was in a bound surface atmosphere. With the observation that the emission is not confined to Io’s disk, Trafton et al. (1974) and Matson et al. (1974) revived the resonant scattering hypothesis. Definitive proof that

resonant scattering is responsible for the sodium emission was provided by Bergstralh et al. (1975) and Trafton et al. (1974) who demonstrated that the sodium intensity is strongly correlated with Io's orbital phase. This is expected for resonantly excited sodium emission because Io's changing radial velocity relative to the sun Doppler shifts the resonant wavelength in and out of the deep solar Fraunhofer line (Figure 1.2). Additional evidence was provided by Macy and Trafton (1975a) who failed to detect emission from Io while it was in eclipse, implying that solar photons are needed to excite the emission. More recently, sodium emission from electron impact excitation has been detected through ground-based spectroscopy (Bouchez et al. 2000) and Galileo spacecraft imaging (Geissler 1999) of Io in eclipse, although this accounts only for only a small fraction of the total emission when Io is in sunlight.

Sodium loss was first assumed to be due to photo-ionization by solar photons (Macy and Trafton 1975a), although they realized that the photo-ionization lifetime is longer than the lifetime to create a complete neutral torus around Jupiter. This conflicted with their observations limiting the cloud to $\sim 1/5$ the circumference of Io's orbit.

A series of papers beginning with Fang et al. (1976) has built up a neutral cloud model as numerical techniques improved and more detailed observations of sodium and the plasma torus became available. The object of these papers has been to understand the evolution of the sodium cloud from the ejection of neutrals out of Io's atmosphere to their eventual loss by ionization. The first of these papers investigated the creation of a torus of neutral sodium originating from a massless Io (Fang et al. 1976). Smyth and McElroy (1977) improved on this by including Io's gravity and limiting the neutral lifetime for a closer agreement with the observations which suggested that the cloud extends only part way around Jupiter. A subsequent paper (Smyth and McElroy 1978) presented the first detailed comparison between models and imaging data (supplied by Murcray and Goody (1978)). The images showed the asymmetric shape of the

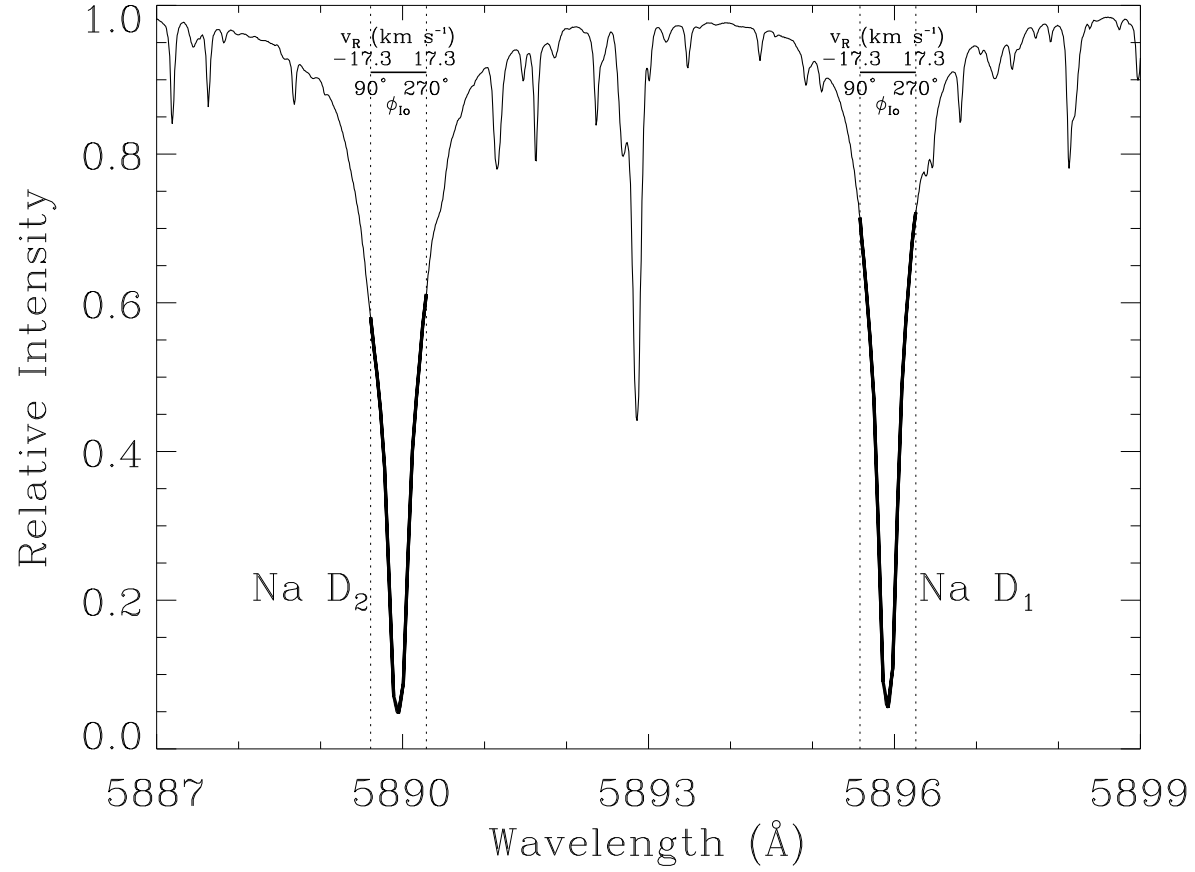


Figure 1.2 The amount of sunlight available for resonant scattering of sunlight by sodium atoms for different Io orbital phases. The intensity of sodium emission is directly proportional to the amount of sunlight at the wavelength of emission in the rest frame of sodium. The radial velocity of Jupiter relative to the sun is taken to be 0 km s⁻¹ here, but must be included when determining actual emission intensity. Scale bars in each line indicate the range of the Doppler shift due to the changes in Io's radial velocity and orbital longitude. This range is also indicated by a heavy line through the part of the solar profile.

sodium cloud: the leading cloud was clearly denser and brighter than the trailing cloud. Assuming a uniform lifetime of $\sim 15 - 20$ hours, they concluded that asymmetric loss from Io could explain the shape of the cloud, noting that ejection of neutrals from the trailing hemisphere primarily populates the forward cloud.

A mechanism for producing the east/west asymmetry (Bergstralh et al. 1975, 1977) in the sodium cloud was explored by Smyth (1979, 1983). The first paper provided a qualitative demonstration that solar radiation pressure on sodium atoms could produce an east/west asymmetry similar to that observed. This work was continued in the second paper with three-dimensional model calculations of the sodium cloud. This work represented a substantial improvement on their ability to model the sodium cloud.

The next major advancement in modeling the neutral clouds came with the development of a general framework for modeling Io's neutral clouds (Smyth and Combi 1988a). The application of this model (Smyth and Combi 1988b) was the first study to include in detail the effects of the plasma torus (although Trafton (1980) had considered the role of the torus in explaining specific observations). These two papers by Smyth and Combi provide the basis for their future work on the neutral clouds and Io's corona: their subsequent work has been applications of this model. These applications include an attempt to use a single source velocity distribution to understand the sodium neutral cloud, the sodium corona, and the fast sodium directional feature (Smyth and Combi 1997) and an application of these results to understanding neutral oxygen observations far from Io (Smyth and Marconi 2000).

1.4 Organization of the Thesis

This thesis is a joint observational and modeling survey of neutral features originating at Io. I concentrate on three distinct but interconnected neutral features: the bound corona, the fast sodium jet, and the extended neutral clouds. Although most of the observations concentrate on sodium due to the relative ease and availability of

observations, I also discuss the physics of oxygen and sulfur lost from Io and compare these species to the well observed sodium features.

The major questions addressed by this thesis are:

(1) Understanding Io's Corona:

- How stable is the corona? Does the corona vary over long time scales?
- Is the corona radially symmetric?
- How does the plasma torus affect the shape of the corona?
- What does the shape of the corona imply about the loss from Io's atmosphere?
- What do morphological differences between the oxygen and sodium coronae imply about loss? Are there differences in the loss mechanisms?

(2) Io's fast sodium jet:

- How large is the source region of the fast sodium jet? Is it a global or narrowly confined region?
- What are the implications of the source size for Io's ionosphere?

(3) The extended neutral clouds:

- Can difference morphological aspects of the clouds be explained through particle motions?
- What effect do the different oxygen and sodium lifetimes have on the neutral clouds?
- How important is the plasma torus in determining the intensity of oxygen? Can column densities be determined without independent measurements of the plasma?

This thesis is organized so as to best answer these questions. In Chapter 2, I discuss the physical processes at work which are common to all three regions. Chapter 3 presents mutual event observations designed to probe the radial structure of the sodium corona. I report the discovery of a previously undetected asymmetry in the column density between the sub-Jupiter and anti-Jupiter hemispheres. Galileo observations of Io's fast sodium jet are described in Chapter 4. These observations are the closest view to date of the source region of the jet. A neutral cloud model based on the model of Wilson and Schneider (1999) and extended for study of sodium cloud to Io is described in Chapter 5. Applications of this model to the corona and extended clouds are presented in Chapters 6 and 7, respectively.